



Photocatalytic inactivation of dual- and mono-species biofilms by immobilized TiO₂

C. Pablos^{a,*}, M. Govaert^b, V. Angarano^b, C. Smet^b, J. Marugán^a, J.F.M. Van Impe^b

^a Department of Chemical and Environmental Technology, ESCET, Universidad Rey Juan Carlos, c/Tulipán s/n, 28933 Móstoles, Madrid, Spain

^b Department of Chemical Engineering, BioTeC+ Chemical and Biochemical Process Technology and Control, KU Leuven, Gebroeders De Smetstraat 1, B-9000 Gent, Belgium

ARTICLE INFO

Keywords:
Biofilms
Photocatalysis
Immobilized TiO₂
TiO₂ nanotubes
Salmonella
Listeria

ABSTRACT

Biofilms formed by different bacterial species are likely to play key roles in photocatalytic resistance. This study aims to evaluate the efficacy of a photocatalytic immobilized nanotube system (TiO₂-NT) (IS) and suspended nanoparticles (TiO₂-NP) (SS) against mono- and dual-species biofilms developed by Gram-negative and Gram-positive strains. Two main factors were corroborated to significantly affect the biofilm resistance during photocatalytic inactivation, i.e., the biofilm-growth conditions and biofilm-forming surfaces. Gram-positive bacteria showed great photosensitivity when forming dual-species biofilms in comparison with the Gram-positive bacteria in single communities. When grown onto TiO₂-NT (IS) surfaces for immobilized photocatalytic systems, mono- and dual-species biofilms did not exhibit differences in photocatalytic inactivation according to kinetic constant values ($p > 0.05$) but led to a reduction of ca. 3–4 log₁₀. However, TiO₂-NT (IS) surfaces did affect biofilm colonization as the growth of mono-species biofilms of Gram-negative and Gram-positive bacteria is significantly ($p \leq 0.05$) favored compared to co-culturing; although, the photocatalytic inactivation rate did not show initial bacterial concentration dependence. The biofilm growth surface (which depends on the photocatalytic configuration) also favored resistance of mono-species biofilms of Gram-positive bacteria compared to that of Gram-negative in immobilized photocatalytic systems, but opposite behavior was confirmed with suspended TiO₂ ($p \leq 0.05$). Successful efficacy of immobilized TiO₂ for inactivation of mono- and dual-species biofilms was accomplished, making it feasible to transfer this technology into real scenarios in water treatment and food processing.

1. Introduction

Biofilm formation has been commonly observed in the water treatment industry as well as many food processing environments, with *Salmonella* and *Listeria* being two pathogenic bacteria that may be considered as relevant for both fields. Biofilms can grow on surfaces, pipelines, and equipment, which leads to biofouling, corrosion, and operational failures. In consequence, it results in reduced efficiency in production and increased energy consumption in operations [1,2]. Biofilm formation in food industries leads to similar problems as well, e.g., it can result in a reduction of the heat transfer in heat exchangers and the optimal circulation of water in cooling towers and potable water systems, which may also reduce the efficiency [3]. In this sector, moreover, biofilms are also responsible for the occurrence of foodborne pathogens on food contact surfaces and food produce.

Bacteria adopt several strategies to survive stressful conditions in the natural environment, including biofilm production. Biofilms are communities of microorganisms that produce extracellular polymeric substances (EPS) to help the cells to anchor themselves to each other and to surfaces such as water pipes. It is well-known that it is much more difficult to inactivate biofilm-associated cells than bacteria in planktonic form and that biofilms represent a challenge for water disinfection and food sanitation [1,2,4].

Photocatalytic water disinfection has been proposed as an alternative to conventional disinfectants such as chlorine, since it can overcome the risk of the formation of disinfection by-products [5]. Other advantages may be that it (i) works at ambient temperature and pressure, (ii) uses air as oxidant without any additional chemicals, and (iii) allows the possibility of using solar light as radiation source. Semiconductor photocatalysis is a process that has been studied for over four decades and

* Corresponding author.

E-mail addresses: crisrina.pablos@urjc.es (C. Pablos), jan.vanimpe@kuleuven.be (J.F.M. Van Impe).

<https://doi.org/10.1016/j.jphotobiol.2021.112253>

Received 17 February 2021; Received in revised form 25 May 2021; Accepted 4 July 2021

Available online 6 July 2021

1011-1344/© 2021 The Authors.

Published by Elsevier B.V. This is an open access article under the CC BY-NC-ND license

(<http://creativecommons.org/licenses/by-nc-nd/4.0/>).

which proved to be very effective against pathogens [2]. When photocatalysts such as titanium dioxide (TiO₂) are irradiated with UV light, powerful oxidizing agents are generated, which are capable of destroying bacteria. It is accepted that the primary mechanism for the photocatalytic destruction of bacteria is based on the attack of their cell wall by hydroxyl radicals ([•]OH) [6,7]. Previous studies have shown that the more complex the cell wall becomes, the more resistant the bacteria are to photocatalytic disinfection. It is not yet known whether the thickness, the structure, and/or the chemistry of the bacterial cell may play a role. Besides, it is even more difficult to understand the entity of each factor, being still under investigation [7,8]. It is, however, well-established that the photocatalytic efficiency depends on the proximity of the photoactivated TiO₂ surface to the cell wall. Suspended nanoparticles of TiO₂, indeed, exhibit a much higher inactivation efficiency as compared to immobilized TiO₂. However, the commercial application of photocatalytic systems obliges the user to employ an immobilized configuration of the photocatalyst, avoiding an additional step to recover the TiO₂ particles [6].

Although the efficacy of the TiO₂ photocatalyst for the inactivation of bacterial suspensions has been widely studied, the inactivation of biofilms has received less attention. To the best of our knowledge, very little has been reported about the photocatalytic efficacy against mono- and dual-species biofilms using lab-scale reactors, therefore this work aims to shed light on this aspect. Moreover, the effects due to inter-species interactions are still unknown. Only some authors have recently evaluated the efficiency of a photocatalytic reactor for inactivation of mono-species biofilms using either TiO₂ in suspension [1,2] or immobilized TiO₂ [4,5,9–11]. Using TiO₂ in suspension in 24-well plates in which *Escherichia coli* biofilms had already been grown, biofilm viability declined after 30 min of irradiation time, as confirmed by a resazurin viability assay based on microbial respiration detection and the plate counting method [1]; whereas *Staphylococcus epidermidis* biofilms required up to 120 min under similar experimental conditions [2]. Regarding the use of immobilized TiO₂, a wide range of different photocatalysts have been tested: i.e., TiO₂-coated glass slides and glass microfiber filters [4], nanostructured oxide-coated carbon steel [11], TiO₂/Ti and TiO₂-Ag/Ti nanotube photoanodes [5], and TiO₂ coated-stainless steel [9]. A varied outcome was also reported in terms of their photocatalytic activity. Photocatalytic properties of coated TiO₂ nanoparticles onto glass surfaces and glass microfiber filters were studied against biofilm-forming bacteria. Although no viable bacterial cells of mono-species biofilms of *Staphylococcus aureus* (Gram-positive) and *Pseudomonas putida* (Gram-negative bacteria) were detected after 120 min, the extracellular polymeric substance (EPS) matrix formed during biofilm colonization remained [4]. It highlights the difficulty of removing the structure of biofilms in the tested self-cleaning surfaces. After 60 min of sunlight irradiation in combination with H₂O₂ (25 mM), a 2-log₁₀ reduction of *Pseudomonas aeruginosa* biofilms was accomplished by nanostructured oxide coatings with photocatalytic activity prepared by Zn acetate (ZnAc) modification [11]. After treatment with TiO₂-glass coated nanoparticles, the viable cell density of *Listeria monocytogenes* biofilms was reduced by up to 3-logs after 90 min of irradiation [9]. Also, highly resistant biofilms of fungi, such as *Candida parapsilosis*, were exposed to photoelectrocatalytic treatment (PEC) when grown onto different surfaces (i.e., PVC, silicone, and PTFE) [5]. After 10 (silicone) and 60 min (PVC and PTFE) of PEC treatment, the fungal biofilm density was reduced by 6-log; whereas PEC-Ag gave rise to a similar reduction after 10 (silicone), 30 (PVC), and 60 min (PTFE) of treatment. Anatase mesoporous titania films were prepared based on the use of the surfactants Brij-58 and compared with nanostructured amorphous titania films. Both were tested against *P. aeruginosa* [12], decreasing the former up to 5 orders of viable bacteria. Cell attachment was also reduced in the former which may be due to a larger size pore of the anatase compared to the amorphous titania films.

This work aimed to explore the antimicrobial capacity of immobilized and suspended TiO₂ against mature biofilms. Moreover,

differences in photocatalytic efficacy were studied between Gram-negative *Salmonella* Typhimurium and Gram-positive *L. monocytogenes* biofilms. As the response of the biofilms to photocatalytic treatment depends on several factors, the interaction exerted between Gram-negative and Gram-positive bacteria in the biofilm was also evaluated by comparing mono- and dual-species biofilms.

2. Materials and Methods

2.1. Bacterial Strains and Growth Conditions

Two bacterial strains were used for the experiments, i.e., *Salmonella enterica* serovar Typhimurium LMG 14933 (ATCC 14028) (Gram-negative) and *Listeria monocytogenes* LMG 23775 (Gram-positive). Both strains were acquired from the Belgium Co-ordinated Collections of Microorganisms (BCCM, Ghent, Belgium). The stock-cultures of these strains were stored at –80 °C in Tryptic Soy Broth (TSB, Becton Dickinson, New Jersey, USA) supplemented with 20% (v/v) glycerol (Scharlab, Barcelona, Spain). For every experiment, a streak plate was prepared by inoculating a loopful of the content of a stock-culture cryovial (*S. Typhimurium* or *L. monocytogenes*) on Luria-Bertani (LB, Becton Dickinson, New Jersey, US) supplemented with 14 g/L of technical agar (VWR international, Pennsylvania, US) and 5 g/L of NaCl (Scharlab, Barcelona, Spain). These plates were incubated for 24 h at 30 °C (*L. monocytogenes*) or 37 °C (*S. Typhimurium*).

2.2. Mono- and Dual-Species Biofilm Formation

Separate precultures were prepared for both microorganisms by transferring one colony from the streak plate into Erlenmeyer flasks containing 20 mL LB broth. Afterward, these flasks were incubated for 24 h at 37 °C or 30 °C for *S. Typhimurium* and *L. monocytogenes*, respectively. After this incubation period, the precultures had a cell concentration of ca. 10⁹ CFU/mL, confirmed by drop plate counting technique. Working cultures were then prepared to reach a cell density of ca. 10⁷ CFU/mL by adding a 100 µL aliquot of the homogenized preculture into 10 mL of optimal medium for biofilm development. Regarding mono-species biofilm formation, 20-fold diluted TSB (Becton Dickinson, New Jersey, USA) and Brain Heart Infusion broth (BHI, VWR international, Pennsylvania, US) were used as optimal medium for *S. Typhimurium* and *L. monocytogenes*, respectively. After homogenization, a specific volume of the working culture was transferred to a sterile contact surface (detailed in Section 2.3) considering a volume to surface area ratio of 0.06 mL/cm² [13]. The inoculated surface was then gently shaken (to cover the entire surface area with the inoculum suspension) and incubated for 24 h at 25 °C (for *S. Typhimurium*) or 30 °C (for *L. monocytogenes*) under static conditions. For the dual-species biofilm formation, a 100 µL aliquot of each homogenized preculture was added to 10 mL of BHI, vortexed, and inoculated onto the surface following the same volume to surface area ratio as mentioned above. Finally, the inoculated surface was incubated under static conditions for 24 h at 30 °C. These optimal dual-species biofilm formation conditions were determined on the basis of some preliminary experiments (data not shown).

After the incubation period of 24 h, a biofilm was formed at the solid-liquid interface. Then, the liquid was discarded, and the contact surface was rinsed three times with sterile Phosphate Buffered Saline (PBS) solution (Sigma-Aldrich, Madrid, Spain) to remove the loosely attached cells. After rinsing, the contact surface was placed in a laminar flow cabinet to dry for ca. 10 min, to avoid that any remaining liquid would interfere during photocatalytic treatment. The biofilms were then ready to undergo the photocatalytic process.

2.3. Photocatalytic Systems and Photocatalysts

The photocatalytic material used in this research was titania (TiO₂).

Titania nanoparticles (suspended in solution, SS) and a coating of titania (TiO_2) nanotubes (immobilized system, IS) were compared. Thus, two TiO_2 photocatalytic systems were studied: (i) TiO_2 nanoparticles (TiO_2 -NP) (SS) in suspension, and (ii) TiO_2 nanotubes (TiO_2 -NT) (IS) grown onto a titanium substrate. (i) The commercial Evonik P25 TiO_2 -NP (SS) (Evonik, Essen, Germany) was used at a concentration of 0.14 g/L, which was optimized in previous studies [7]. (ii) The TiO_2 nanotubes (TiO_2 -NT) (IS) forming the coating were obtained by galvanostatic anodization (2.7–36.8 V, 1.8 mA/cm²) of Ti foil according to the protocol of Mena et al. [14]. The nanotube diameter determined by SEM micrographs corresponded to 99.1 ± 9.2 nm [14]. The anodized foil was then cut into rectangular pieces of 2 cm² representing the biofilm contact surface.

TiO_2 -NP (SS) and TiO_2 -NT (IS) were tested to inactivate mono-species and dual-species biofilms developed by *S. Typhimurium* (Gram-negative) and/or *L. monocytogenes* (Gram-positive). To test TiO_2 -NP (SS), biofilms were grown at the bottom of a borosilicate glass beaker corresponding to an area of 20 cm². To test the immobilized system, biofilms were grown on the 2 cm² pieces of TiO_2 -NT (IS). In this case, the rinsed and dried biofilms were placed at the bottom of a borosilicate glass beaker. 150 mL of sterile PBS was added, either with TiO_2 -NP (SS) or without, in the case of TiO_2 -NT (IS), and the photocatalytic treatment took place while stirring.

The biofilms were placed facing a Philips TL 6 W black light lamp with a maximum emission peak centered and full width at half maximum at 365/20 nm. Biofilms in suspended and immobilized photocatalytic systems received a similar UV-A irradiation, which corresponded to an irradiance of 8.64 W/m². The system was equilibrated for 5 min, and in the meantime, the lamp was switched on to stabilize its irradiance before the treatment started and, afterward, placed to irradiate the beaker.

Control experiments (negative controls) were carried out to discard any inactivation effect due to pure UV-A radiation exposure and as a consequence of the photocatalyst alone. These control experiments aimed to guarantee that the inactivation effect was due to the combined effect of the photocatalyst and UV-A radiation. For this reason, two negative control experiments were performed: (i) Dark control experiments in the presence of the photocatalyst, either suspended TiO_2 (TiO_2 -NP) (SS) or immobilized TiO_2 -NT (IS) (Dark: – UV-A, + Photocatalyst), and (ii) photolysis control experiments in the presence of UV-A light in

the absence of the photocatalyst (Photolysis: + UV-A, – Photocatalyst). The photolysis control experiment for the immobilized TiO_2 -NT (IS) was performed using a 2 cm² of non-anodized Ti foil was used instead of TiO_2 -NT (IS) as biofilm contact surface.

In Fig. 1, a schematic representation of both configurations of photocatalysts has been included, as well as a photographic image of both photocatalytic set-ups used.

2.4. Quantification of Viable Biofilm Cells

The viable cells within the biofilm were quantified every 60 min throughout the experiment with a total treatment time of 240 min. As this quantification method is destructive, a different beaker and biofilm were used for each treatment time. Moreover, the cell density of the untreated biofilms ($t = 0$ min) was also determined.

For the viable cells quantification, the PBS suspension was removed. The biofilms placed either onto the bottom glass beaker (TiO_2 -NP (SS)) or onto the coating of titania (TiO_2 -NT (IS)) were left to dry in a laminar flow cabinet. After drying, 2 mL of sterile PBS was added and biofilms were detached from the surface with a scraper (Scharlab, Barcelona, Spain) for the viable cell counting. Viable cells from the obtained suspension were enumerated for each bacterial strain after making serial dilutions using sterile saline solution (0.85% (w/v) NaCl, Scharlab, Barcelona, Spain). The drop plate counting technique was used by spotting 10 μL of each decimal dilution four times onto agar plates. For longer irradiation times (low bacterial cell density) higher volumes (100–1000 μL) of the undiluted suspension were also plated to reduce the limit of detection to 1 CFU/mL or 0 log₁₀ (CFU/mL). Therefore, the final detection limit was 1 CFU/cm².

General and selective agar media were used for the mono- and dual-species biofilms, respectively. TSB (Becton Dickinson, New Jersey, USA) supplemented with 14 g/L of technical agar (VWR international, Pennsylvania, US) was always used as general medium. Xylose Lysine Deoxycholate agar (XLD, Merck & Co, New Jersey, US) and PALCAM *L. monocytogenes* selective agar (VWR International, Pennsylvania, US) were used as selective media for *S. Typhimurium* and *L. monocytogenes*, respectively. General medium plates were, on the one hand, incubated for 24 h at 37 °C for the *S. Typhimurium* mono-species biofilms. For the *L. monocytogenes* mono-species biofilms, on the other hand, general medium plates were incubated at 30 °C for 48 h. Finally, XLD plates

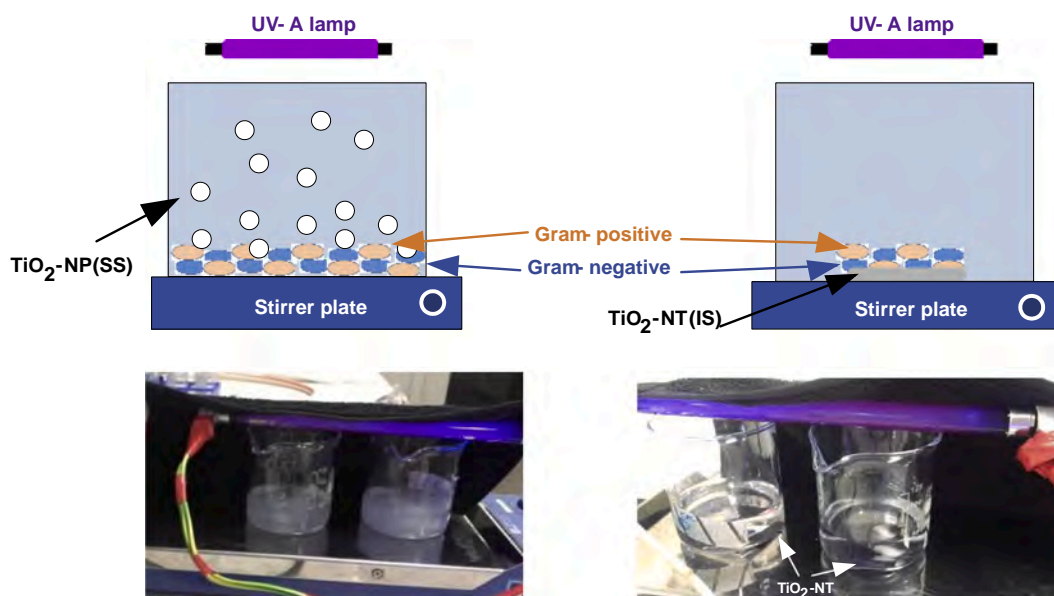


Fig. 1. Schematic representation and photographic images of suspended (TiO_2 -NP) (SS) (left) and the immobilized (TiO_2 -NT) (IS) (right) photocatalytic configurations tested for the inactivation of dual-species biofilms.

were always incubated at 37 °C for 24 h, whereas PALCAM plates were always incubated at 30 °C for 48 h.

The methodology as described so far, is summarized in Fig. 2.

2.5. Disinfection Kinetic Constant

The disinfection kinetic constant (k) obtained by the classical Chick–Watson log-linear model (Eq. 1) [15] has been chosen to establish a comparison of the photocatalytic cell density inactivation rates obtained for the different photocatalytic systems and biofilm-growth conditions. In the equation.

$$\log N/N_0 = -kt \quad (1)$$

N_0 ($\log_{10}\text{CFU}/\text{cm}^2$) represents the initial viable bacterial cell density; N ($\log_{10}\text{CFU}/\text{cm}^2$) is the surviving viable bacterial cell density after time t (min), and k represents the disinfection rate constant (min^{-1}).

2.6. Statistical Analysis

All experiments were performed in triplicate, i.e., three independent biological replicates were used and means calculated. All statistical analyses were performed using the Statgraphics 18 software (Statistical Graphics, Washington, USA). two-way analysis of variance (ANOVA) and Fisher's Least Significant Difference (LSD) tests were used to distinguish which means were significantly different from others. A confidence level of 95.0% ($\alpha = 0.05$) was applied. Thus, data were considered significantly different at $p \leq 0.05$. Firstly, ANOVA tests were performed to determine whether there were any significant differences amongst means of logarithmic initial viable counts of *S. Typhimurium*

and *L. monocytogenes* because of growing within either mono- or dual-species biofilms and onto different colonization surfaces depending on the photocatalytic system, suspended TiO_2 -NP (SS), and immobilized, TiO_2 -NT (IS). In the second part of this study, ANOVA tests were again used to determine whether there were significant differences amongst photocatalytic inactivation kinetic constants obtained for *S. Typhimurium* and *L. monocytogenes* because of growing within either mono- or dual-species biofilms and depending on the photocatalytic treatment performed, either TiO_2 -NP (SS) or TiO_2 -NT (IS). Significant differences amongst photocatalytic inactivation kinetic constants were indicated with different (uppercase) letters with "A" indicating the lowest value.

3. Results & Discussion

3.1. Photocatalytic Inactivation of Mono-Species Biofilms

The behavior of mono-species biofilms of two strains with structural differences, i.e., Gram-negative *S. Typhimurium* and Gram-positive *L. monocytogenes*, was evaluated with respect to their ability to form biofilms and their resistance to photocatalytic inactivation.

3.1.1. Photocatalytic Inactivation of Gram-Negative Bacteria

The inactivation results for the mono-species *S. Typhimurium* biofilms are depicted in Figs. 3 and 4 for the suspended, TiO_2 -NP (SS), and immobilized, TiO_2 -NT (IS) photocatalytic system, respectively. The initial cell density of the *S. Typhimurium* biofilms corresponded to ca. $5 \pm 1 \log_{10}$ (CFU/cm^2) when using TiO_2 in suspension (TiO_2 -NP) (SS) (Fig. 3), whereas ca. $3.5 \pm 0.5 \log_{10}$ was attained with immobilized TiO_2 (TiO_2 -NT) (IS) (Fig. 4). These initial values are equivalent to an

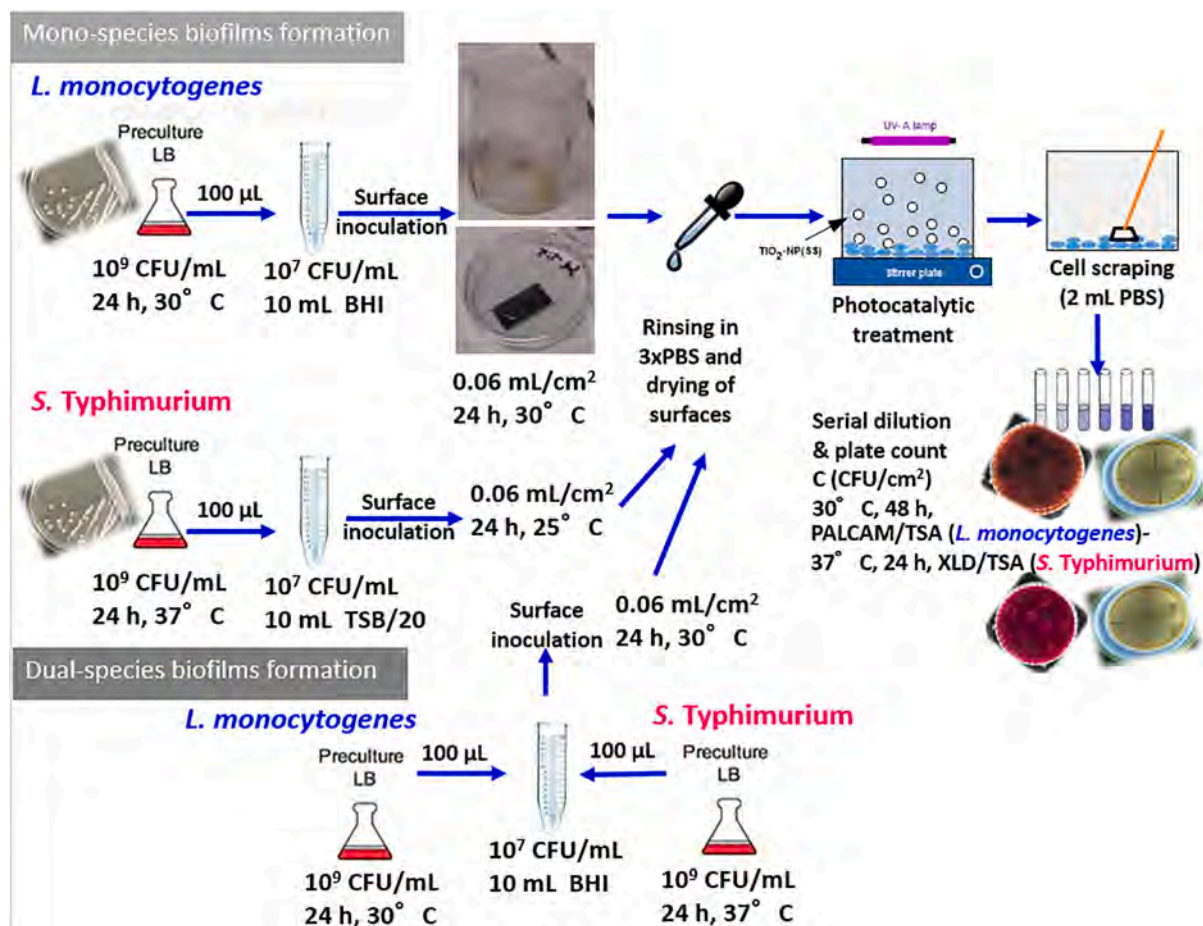


Fig. 2. Schematic representation of mono- and dual-species biofilm formation, inactivation and quantification.

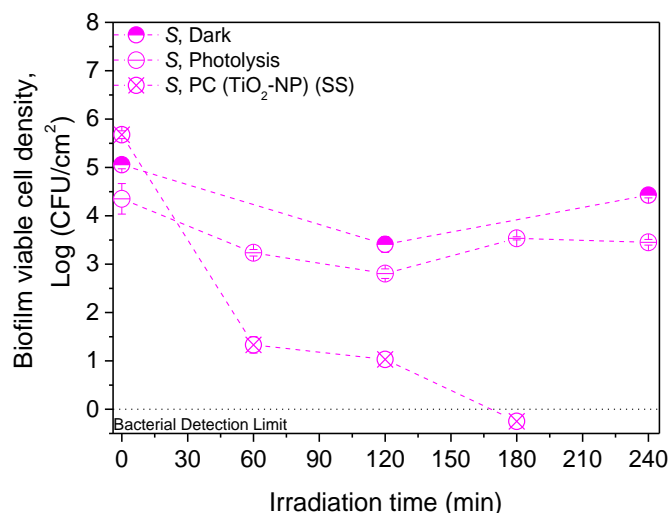


Fig. 3. Inactivation curves of mono-species biofilms of *S. Typhimurium* in a photocatalytic system with TiO_2 in suspension ($\text{TiO}_2\text{-NP}$) (SS). TiO_2 concentration: 0.14 g/L. S: *S. Typhimurium*. Dark: + $\text{TiO}_2\text{-NP}$ (SS), - UV-A. Photolysis: - $\text{TiO}_2\text{-NP}$ (SS), + UV-A. Photocatalysis (PC): + $\text{TiO}_2\text{-NP}$ (SS), + UV-A. Values represent the mean \pm SD of three independent assays.

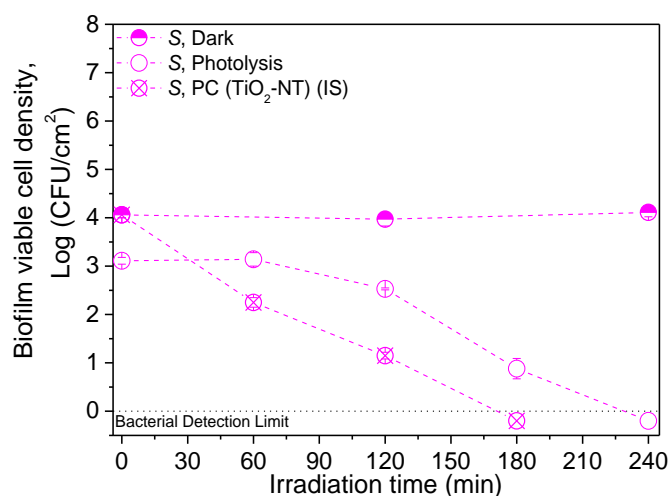


Fig. 4. Inactivation curves of mono-species biofilms of *S. Typhimurium* in a photocatalytic system with immobilized TiO_2 ($\text{TiO}_2\text{-NT}$) (IS). S: *S. Typhimurium*. Dark: + $\text{TiO}_2\text{-NT}$ (IS), - UV-A. Photolysis: - $\text{TiO}_2\text{-NT}$ (IS), + UV-A. Photocatalysis (PC): + $\text{TiO}_2\text{-NT}$ (IS), + UV-A. Values represent the mean \pm SD of three independent assays.

irradiation time equal to zero. An approximate 6- \log_{10} (CFU/cm²) reduction of the viable *S. Typhimurium* cell density was photocatalytically achieved after 180 min of irradiation when using TiO_2 in suspension. It is important to note that a 4- \log_{10} (CFU/cm²) reduction was observed for *S. Typhimurium* by immobilized TiO_2 ($\text{TiO}_2\text{-NT}$) (IS) for the same treatment time.

3.1.2. Photocatalytic Inactivation of Gram-Positive Bacteria

Inactivation of the *L. monocytogenes* mono-species biofilms was displayed in Figs. 5 and 6 for the suspended ($\text{TiO}_2\text{-NP}$) (SS) and immobilized ($\text{TiO}_2\text{-NT}$) (IS) photocatalytic system, respectively. For both systems, the initial viable cell density of the mature *L. monocytogenes* model biofilms corresponded to ca. $5.0 \pm 0.1 \log_{10}$ (CFU/cm²). This concentration thus corresponded to an irradiation time equal to zero.

Gram-positive *L. monocytogenes* were completely inactivated only when illuminated suspended TiO_2 ($\text{TiO}_2\text{-NP}$) (SS) was used, as no

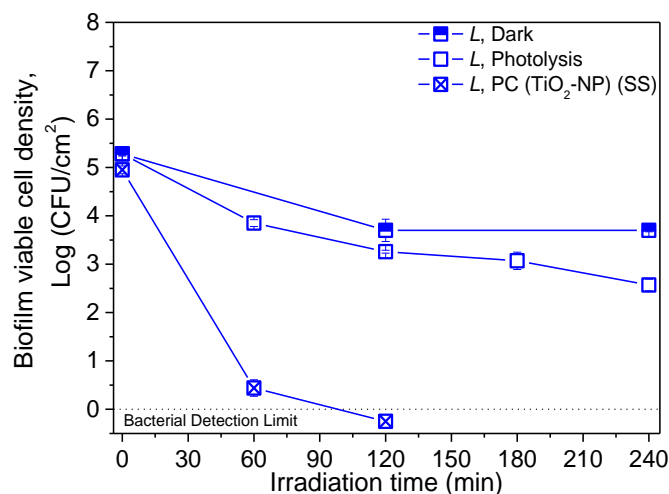


Fig. 5. Inactivation curves of mono-species biofilms of *L. monocytogenes* in a photocatalytic system with TiO_2 in suspension ($\text{TiO}_2\text{-NP}$) (SS). TiO_2 concentration: 0.14 g/L. L: *L. monocytogenes*. Dark: + $\text{TiO}_2\text{-NP}$ (SS), - UV-A. Photolysis: - $\text{TiO}_2\text{-NP}$ (SS), + UV-A. Photocatalysis (PC): + $\text{TiO}_2\text{-NP}$ (SS), + UV-A. Values represent the mean \pm SD of three independent assays.

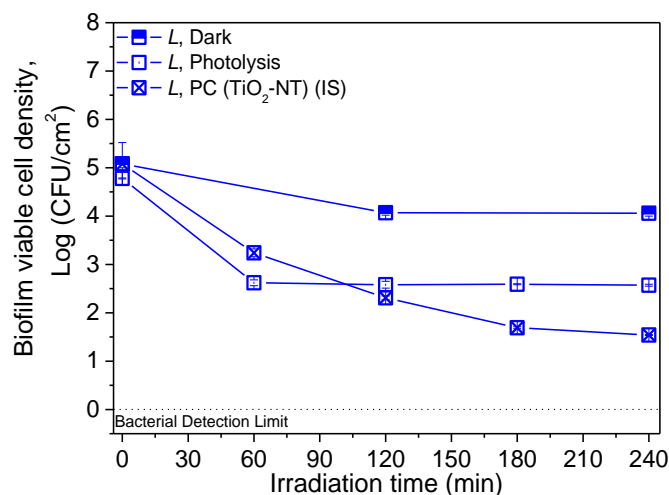


Fig. 6. Inactivation curves of mono-species biofilms of *L. monocytogenes* in a photocatalytic system with immobilized TiO_2 ($\text{TiO}_2\text{-NT}$) (IS). L: *L. monocytogenes*. Dark: + $\text{TiO}_2\text{-NT}$ (IS), - UV-A. Photolysis: - $\text{TiO}_2\text{-NT}$ (IS), + UV-A. Photocatalysis (PC): + $\text{TiO}_2\text{-NT}$ (IS), + UV-A. Values represent the mean \pm SD of three independent assays.

significant effect on inactivation is observed when the dark and photolysis controls were performed. A 5- \log_{10} (CFU/cm²) reduction was observed with the $\text{TiO}_2\text{-NP}$ (SS) system after 120 min of irradiation. A similar reduction was obtained by Buck et al. [2] when biofilms of *S. epidermis* were exposed for 120 min to irradiation with 1 g/L Degussa (Evonik) P25 TiO_2 in 24-well plates with a total working volume of 400 μL .

The immobilized photocatalyst $\text{TiO}_2\text{-NT}$ (IS) led to a 3- \log_{10} reduction of the *L. monocytogenes* biofilms after 120 min of irradiation. This is lower efficiency than that of TiO_2 in suspension ($\text{TiO}_2\text{-NP}$) (SS), but still very promising.

Hence, the immobilized photocatalyst $\text{TiO}_2\text{-NT}$ (IS) resulted in high efficiency in terms of inactivation of mono-species biofilms of *S. Typhimurium* (4- \log_{10} reduction) and *L. monocytogenes* (3- \log_{10} reduction). These reductions are similar or even higher than those reported by other authors such as Jalvo et al. [10], who reached 2- \log_{10} removal of

the total biomass using immobilized TiO₂ with self-cleaning purposes. Li and Cheng [11] tested nanostructured oxide coatings on steel surface prepared by anodization and treated by Zn acetate prior to annealing to include ZnFe₂O₄ as active photocatalytic material under sunlight. The photocatalytic activity of this material was evaluated under sunlight radiation to inactivate *P. aeruginosa* bacteria and biofilms leading to more than 2-log₁₀ reduction (99.6%) of bacterial concentration due to the formation of superoxide anion O₂⁻ and holes (h⁺). The addition of UV-60 min and 0.2 mM H₂O₂ was required to remove residual dead cells and residual biofilm increasing the yield rate of O₂⁻ and the formation of hydroxyl radicals resulting in a biomass removal efficiency of also 2-log₁₀ (99.3%). To the best of the authors' knowledge, only Pires et al. [5] accomplished a 6-log₁₀ reduction of the viable cell density of fungal biofilms after 10–60 min of irradiation (depending on the growth surface) when using photoanodes of titania nanotubes of diameter of 150 ± 10 nm, TiO₂-NT/Ti and TiO₂-NT-Ag/Ti, under a bias potential of +1.5 V. For photocatalytic experiments, the outcome was a 6-log₁₀ reduction of fungal biofilms after 10, 60, and 120 min using biofilms developed onto silicone, PTFE, and PVC, respectively. Therefore, fungal attachment to PVC was stronger as compared to the other materials due to different properties of the growth surface, such as roughness, charge, and hydrophobicity. Despite the fact that the fungi cell wall differs from the bacterial cell wall, by presenting a thicker cell wall with a higher density and complexity, fungal biofilms were totally eradicated.

Immobilized systems have widely been reported to lead to mass transfer limitations and lower titania surface area which results in reduced radiation absorption and hydroxyl radical generation rates [6]. Moreover, Pablos et al. [6] also reported how bacteria–catalyst interaction can be affected by the use of either a suspension or immobilized TiO₂. In this case, particles of TiO₂ in suspension can cover most of the external wall of the bacteria in the biofilm formed on the bottom of the beaker, and the smallest can even access the cytoplasm. In this immobilized TiO₂ system, biofilms were grown onto the nanotubes titania surface, hence, the contact bacteria–TiO₂ takes place in a reduced fraction of the biofilm, excluding the possibility of accessing titania particles through the bacterial cell wall. Thus, the attacks to the bacteria are likely to be concentrated on a specific area of the immobilized TiO₂ system, whereas the damages produced by TiO₂ in suspension would be distributed all over the bacterial cell wall. Additional accumulation of bacteria onto titania surface during biofilm formation may also represent a barrier for the release of free radicals from the photocatalytic surface.

Since the hydroxyl radical attack occurs at the outer cell wall of the bacterial cells, the difference in cell wall structure between Gram-positive and Gram-negative cells may explain the observed differences in photocatalytic inactivation efficiency. In general, greater resistance of Gram-positive bacteria to photocatalytic disinfection has widely been observed as compared to Gram-negative bacteria, which is deemed to be the result of the thicker cell wall of Gram-positive bacteria. Nevertheless, this is still under debate as other authors claimed that the complexity of the cell wall of Gram-negative bacteria might also compromise the efficiency of the photocatalytic inactivation [7]. In the case of biofilm inactivation, also the ability of each strain to form EPS matrices rich in exopolysaccharides depending on the strain itself, cultivation method, maturity of the biofilm, and grown surface, must be considered as they are likely to hinder the photocatalytic attack.

Within this study, a certain effect of photo-inactivation on biofilms of *S. Typhimurium*, and to a lesser extent of biofilms of *L. monocytogenes*, was observed only when these strains grew onto Ti foil for the photolytic experiment (Figs. 4 and 6). In fact, in TiO₂-NT (IS) systems, the photolytic effect is much more pronounced than the photocatalytic inactivation. Moreover, when grown onto TiO₂-NT (IS) for the photocatalytic experiments, biofilms of Gram-positive bacteria showed higher resistance to be inactivated in comparison with Gram-negative bacteria. In contrast, the opposite behavior was observed in Figs. 3 and 5. A suspended TiO₂ based photocatalytic treatment (TiO₂-NP) (SS) of mono-

species biofilms of Gram-positive bacteria turned out to be more efficient than the corresponding photocatalytic treatment of Gram-negative bacteria ($p \leq 0.05$). Thus, it can be concluded that the growth surface of biofilms and the microbial attachment did play a significant role in their response to photolytic and photocatalytic treatment, which is different for each photocatalytic configuration.

Actually, other authors have also reported differences in photocatalytic efficacy and cell attachment due to the pore size, roughness, hydrophobicity, etc. provided by the colonization surface [12]. Others did not see differences in colonization ability but did in biovolume of biofilm [16]. Others as Pezzoni et al. [12] also observed the anti-adhesion properties of some surfaces due to differences in pore size. Although TiO₂-NT (IS) and Ti foil did not seem to affect colonization ability of *L. monocytogenes*, *S. Typhimurium* colonization was significantly impaired on these surfaces compared to that of TiO₂-NP (SS). Thus, TiO₂-NT (IS) and Ti foil as biofilm grown surface may induce stress during biofilm formation to both mono-species biofilms which may increase their photosensitivity to UV-A radiation.

3.2. Photocatalytic Inactivation of Gram-Negative and Gram-Positive Dual-Species Biofilms

Interspecies interactions of multi-species biofilms may differ from the physiology of mono-species biofilms, possibly showing different behavior against photocatalytic disinfection. As cell-to-cell interactions may play a key role in cell colonization and resistance against disinfection, the effect of photocatalytic treatment was not only studied for commonly used mono-species biofilms, but also for more complex dual-species biofilms.

Figs. 7 and 8 show the inactivation results of dual-species biofilm communities of both Gram-negative and Gram-positive bacteria expressed in log₁₀ (CFU/cm²) when using suspended (TiO₂-NP) (SS) (Fig. 7) and immobilized TiO₂ (TiO₂-NT) (IS) (Fig. 8).

Firstly, it should be noticed that the initial viable cell density of *S. Typhimurium* and *L. monocytogenes* in the dual-species model biofilms was higher ($6 \pm 1 \log_{10}$ CFU/cm²) when grown onto a borosilicate glass surface (TiO₂-NP) (SS) as compared to either the Ti foil or the immobilized system (TiO₂-NT) (IS). For the immobilized system, the initial viable cell densities of the two bacteria within the biofilms were ca. 3 log₁₀ CFU/cm². No competitive interactions between *S. Typhimurium*

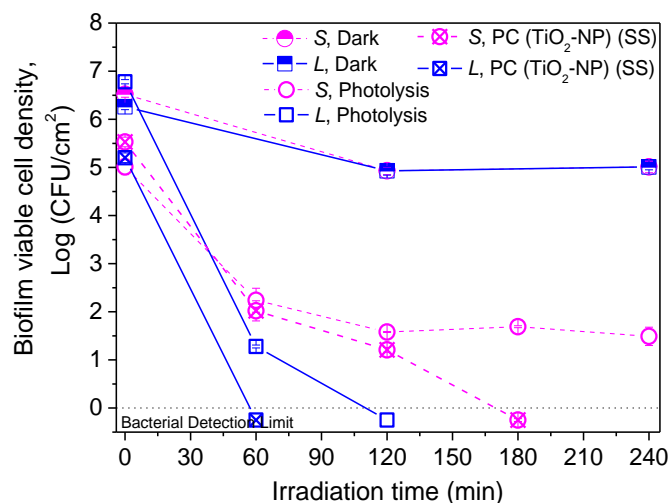


Fig. 7. Inactivation curves of the dual-species biofilms of *S. Typhimurium* and *L. monocytogenes* in a photocatalytic system with TiO₂ in suspension (TiO₂-NP) (SS). TiO₂ concentration: 0.14 g/L. S: *S. Typhimurium*. L: *L. monocytogenes*. Dark: + TiO₂-NP (SS), - UV-A. Photolysis: - TiO₂-NP (SS), + UV-A. Photocatalysis (PC): + TiO₂-NP (SS), + UV-A. Values represent the mean ± SD of three independent assays.

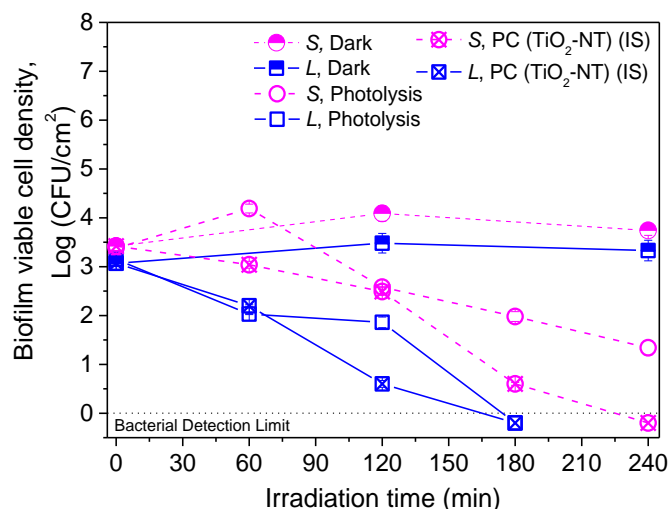


Fig. 8. Inactivation curves of the dual-species biofilms of *S. Typhimurium* and *L. monocytogenes* in a photocatalytic system with immobilized TiO_2 ($\text{TiO}_2\text{-NT}$) (IS). S: *S. Typhimurium*. L: *L. monocytogenes*. Dark: + $\text{TiO}_2\text{-NT}$ (IS), - UV-A. Photolysis: - $\text{TiO}_2\text{-NT}$ (IS), + UV-A. Photocatalysis (PC): + $\text{TiO}_2\text{-NT}$ (IS), + UV-A. Values represent the mean \pm SD of three independent assays.

and *L. monocytogenes* seemed to occur when they were co-cultured as both microorganisms presented similar initial viable cell density values when they were part of the dual-species biofilm. However, dual-species biofilm formation was significantly ($p \leq 0.05$) less favored onto $\text{TiO}_2\text{-NT}$ (IS) and Ti foil. In addition, the ability of *S. Typhimurium* to form dual-species biofilms onto $\text{TiO}_2\text{-NT}$ (IS) and Ti foil (photolysis control) was significantly ($p \leq 0.05$) lower than its ability to form mono-species biofilms (Figs. 4 and 8). For *L. monocytogenes*, the initial viable cell density was not significantly ($p > 0.05$) different between the mono-species and the dual-species model biofilms grown onto the borosilicate glass surface (Figs. 5 and 7). However, as for *S. Typhimurium*, the ability of *L. monocytogenes* to form mono-species biofilms onto $\text{TiO}_2\text{-NT}$ (IS) and Ti foil was significantly ($p \leq 0.05$) favored over the dual-species biofilm formation (Figs. 6 and 8). Again, these results revealed the influence of the growth surface on the ability of the cells to form biofilms, which is different for each photocatalytic configuration, seeming $\text{TiO}_2\text{-NT}$ (IS) and Ti foil to provide antibiofouling properties. Besides this, the fact that the dual-species viable cell density is most of the times lower than the corresponding single-species viable cell density for $\text{TiO}_2\text{-NT}$ (IS) and Ti foil ($p \leq 0.05$) may also be related to competitive interactions, affecting microbial attachment, and giving rise to waste components which may be toxic for other species [16].

The dark control experiment showed that the viable cell density of the dual-species biofilms did not significantly decrease as a function of the treatment time, and this for both photocatalytic configurations (Figs. 7 and 8).

When forming dual-species biofilms, the *S. Typhimurium* and *L. monocytogenes* population seemed to be inactivated by UV-A light (photolysis) for both (i) $\text{TiO}_2\text{-NP}$ (SS) and (ii) $\text{TiO}_2\text{-NT}$ (IS). (i) For $\text{TiO}_2\text{-NP}$ (SS), the Gram-positive *L. monocytogenes* population showed much greater photosensitivity in comparison to the Gram-negative *S. Typhimurium* population. The *L. monocytogenes* population grown onto borosilicate glass at the bottom of the photoreactor corresponds to ca. $7 \log_{10}$ (CFU/cm²), and it was totally photo-inactivated after 120 min of irradiation (Fig. 7). For the *S. Typhimurium* biofilms, also a complete photo-inactivation corresponding to a $5.5 \log_{10}$ reduction was achieved. However, a treatment time of 180 min of irradiation was required (Fig. 7). This result was totally opposed to that observed when forming mono-species biofilms for $\text{TiO}_2\text{-NP}$ (SS) since *S. Typhimurium* and *L. monocytogenes* did not show sensitivity to the photolytic treatment (Figs. 3 and 5). (ii) For $\text{TiO}_2\text{-NT}$ (IS), when the dual-species biofilm was

formed onto a Ti foil, an initial *L. monocytogenes* viable cell density of $3 \log_{10}$ (CFU/cm²) was completely photo-inactivated within 180 min (Fig. 8). On the contrary, the *S. Typhimurium* population, corresponding to $3.5 \log_{10}$, was not totally photo-inactivated, but only a $2 \log_{10}$ reduction was achieved after 240 min of irradiation (Fig. 8). Only when these strains grew onto Ti foil for the photolytic experiment (Figs. 4 and 6), a certain effect of photo-inactivation on mono-species biofilms of *S. Typhimurium*, and to a lesser extent of mono-species biofilms of *L. monocytogenes*, was detected as mentioned in Section 3.1.2. Thus, apart from the suggested induced stress in biofilm formation by $\text{TiO}_2\text{-NT}$ (IS) and Ti foil, competition interactions between both strains of bacteria seems to be occurring in the two systems, $\text{TiO}_2\text{-NP}$ (SS) and $\text{TiO}_2\text{-NT}$ (IS), resulting in increased bacterial photosensitivity. It must also be noticed that other authors as Govaert et al. [17] and Haddad et al. [18] have reported a particular spatial distribution of dual-species biofilms of *L. monocytogenes* and *S. Typhimurium*. They observed that Gram-negative bacteria were mostly situated on the top meanwhile Gram-positive bacteria were placed at the bottom of the biofilm. Considering this finding, it had been expected lower photosensitivity of *L. monocytogenes* towards UV-A radiation compared to *S. Typhimurium* as the latter would be able to protect the former from direct UV-A radiation. Thus, competition interactions between both strains of bacteria forming the dual-species biofilm seemed to be taking place, resulting in the weakening of *L. monocytogenes* against UV-A radiation.

The photocatalytic treatment showed different effects depending on the photocatalytic system. First, the $\text{TiO}_2\text{-NP}$ (SS) is discussed and, afterward, the TiO_2 ($\text{TiO}_2\text{-NT}$) (IS) is evaluated. In each of these two discussions, a comparison between dual-species biofilms and mono-species biofilms is considered. The photocatalytic treatment with TiO_2 in suspension ($\text{TiO}_2\text{-NP}$) (SS) showed effective inactivation for both *S. Typhimurium* and *L. monocytogenes* in the dual-species biofilm after 180 and 60 min of irradiation, respectively (Fig. 7). However, a longer irradiation time was required to reach a total photocatalytic inactivation of mono-species biofilms of *L. monocytogenes* (120 min), whereas a similar time was required in the case of *S. Typhimurium* (180 min), despite both presented a similar initial viable cell density of ca. $5 \log_{10}$ (Figs. 3 and 5).

When the dual-species biofilm was formed onto immobilized TiO_2 ($\text{TiO}_2\text{-NT}$) (IS), a $3 \log_{10}$ reduction of the *L. monocytogenes* population was obtained following 180 min of photocatalytic treatment. Since similar \log_{10} -reduction values were obtained using UV-A light only (photolysis), there was no photocatalytic enhancement of *L. monocytogenes* inactivation in the dual-species model biofilm in $\text{TiO}_2\text{-NT}$ (IS). Thus, hydroxyl radical attack did not seem to be occurring. However, considering the above-mentioned spatial distribution of both strains in dual-species biofilms, if *L. monocytogenes* had mainly been placed at the bottom layer of the biofilm, it should have been affected by $\bullet\text{OH}$ radicals formed at the photocatalytic surface. This may be due to the protection provided by EPS matrix. Fig. 9 depicts a schematic representation of the photocatalytic attack expected to happen for $\text{TiO}_2\text{-NP}$ (SS) and $\text{TiO}_2\text{-NT}$ (IS). On the contrary, the possibility of diffusion of titania nanoparticles in $\text{TiO}_2\text{-NP}$ (SS) systems through the biofilm (as explained in Section 3.1.2) seemed to facilitate the photocatalytic attack in both bacterial strains in dual- and mono-species biofilms. For the *S. Typhimurium* population, on the other hand, a photocatalytic effect was observed since the photocatalytic treatment resulted in complete inactivation of the *S. Typhimurium* population (i.e., a $3 \log_{10}$ reduction) after 240 min of photocatalytic treatment with $\text{TiO}_2\text{-NT}$ (IS), which was not the case while using UV-A only (photolysis). According to the described spatial distribution of *S. Typhimurium* in the dual-species biofilm, as the Gram-negative bacteria is supposed to be at the top part of the biofilm, it may not have such a direct contact to holes (h^+) and hydroxyl radicals (OH) but being directly intercepted by UV-A radiation may also induce some stress. Thus, further investigations are required to elucidate the photocatalytic inactivation mechanism existing in dual-species biofilms. When forming mono-species biofilms, the

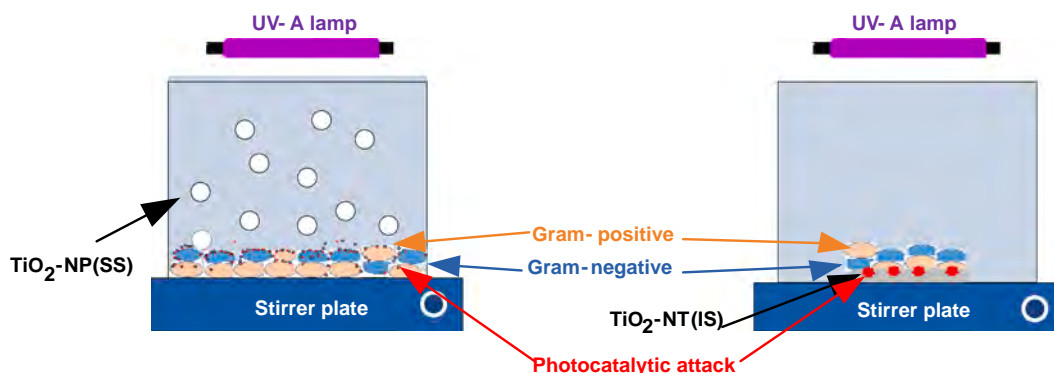


Fig. 9. Schematic representation of the photocatalytic attack in the suspended ($\text{TiO}_2\text{-NP}$) (SS) (left) and the immobilized ($\text{TiO}_2\text{-NT}$) (IS) (right) photocatalytic systems tested for the inactivation of dual-species biofilms.

total *S. Typhimurium* population was photocatalytically inactivated after 180 min (i.e., a 4- \log_{10} reduction). Only a 3- \log_{10} reduction of mono-species biofilms of *L. monocytogenes* with an initial viable cell density of ca. 5- \log_{10} was observed after 240 min of photocatalytic treatment (Figs. 4 and 6, respectively). Thus, despite that the immobilized photocatalytic system required a longer treatment time than TiO_2 in suspension, it allowed the complete inactivation of Gram-negative and Gram-positive bacteria present in the dual-species biofilms. Similar results were obtained for mono-species biofilms of *S. Typhimurium*, giving rise to a complete inactivation (4- \log_{10} reduction). Despite that a total inactivation was not observed for the mono-species biofilms of *L. monocytogenes*, a noticeable reduction of 3- \log_{10} was attained.

In the first part of this study, greater resistance of Gram-positive mono-species biofilms was observed as compared to Gram-negative mono-species biofilms in immobilized photocatalytic systems ($\text{TiO}_2\text{-NT}$) (IS). Under co-culturing conditions (Figs. 7 and 8), Gram-positive bacteria showed a significantly higher sensitivity to the photolytic treatment than the *S. Typhimurium* cells, which was not observed for the mono-species biofilms in $\text{TiO}_2\text{-NP}$ (SS) and $\text{TiO}_2\text{-NT}$ (IS). This work corroborates that cooperation, competition, or neutral interactions most likely occurred between species, which was previously claimed by other researchers [16–19]. Multi-species biofilms may exhibit different interactions in comparison with mono-species biofilms, which may influence their relative resistance to photolytic and photocatalytic treatment. In this case, co-culturing of *L. monocytogenes* with *S. Typhimurium* as a dual-species biofilm resulted in a greater sensitivity of *L. monocytogenes* against UV-A radiation, involving a competitive interaction between both microorganisms. Although studied to a lesser extent, it has also been reported that dual-species biofilms are considered to be more resistant to antimicrobials than mono-species biofilms due to the particular distribution of Gram-negative and Gram-positive strains of bacteria mentioned above [16–18,20,21]. Being Gram-positive bacteria mainly in the bottom part of the biofilm, they are likely to be protected from Gram-negative bacteria on the top from the attack of chemical and physical disinfectant agents. Haddad et al. [18] also determined that by itself *L. monocytogenes* developed less EPS, but in combination with Gram-negative *Pseudomonas fluorescens*, *L. monocytogenes* enhanced a greater production of EPS by *P. fluorescens*. The resistance mechanisms involved may be based on nutrients availability and colonization ability, quorum sensing response, etc., but still remain unclear. Nevertheless, this finding regarding the Gram-type and resistance does not correlate with the depicted experimental data and some related in the literature. Gkana et al. [22], Iñiguez-Moreno et al. [23], Li et al. [24] also concluded that mixed-population biofilms of either (i) Gram-negative and Gram-positive bacteria or (ii) Gram-positive bacteria and fungi were more sensitive to disinfectants, chemical agents and extracts (such as sodium chloride, benzalkonium chloride, peracetic acid, curcumin, etc.) as compared to mono-species

biofilms. Govaert et al. [17] despite also reporting this particular spatial distribution of *L. monocytogenes* and *S. Typhimurium* within the dual-species biofilms also demonstrated higher sensitivity of *L. monocytogenes* to Cold Atmospheric Plasma (CAP). They also explained this behavior by the description of the occurrence of competitive interactions between both strains of bacteria due to e.g., waste accumulation, production of inhibitory agents, nutrient limitations, matrix-degrading enzymes, produced by one of the species. Kostaki et al. [25] and Puga et al. [26] noted opposite tendencies depending on the target disinfectant (hydrogen peroxide-peracetic acid mixtures and enzymatic treatment, respectively).

3.3. Kinetic Constant Evaluation of Photocatalytic Inactivation Efficiency of Suspended Nanoparticles and Immobilized Nanotubes of TiO_2

The Chick–Watson log-linear model was fitted to the data related to the photocatalytic processes (photocatalytic data in Figs. 3–8). The log-linear models fitted to the data are included in the Supplementary Material (Figs. 1–6). The disinfection kinetic constants, k , were estimated and are displayed in Table 1 for the mono- and dual-species biofilms, and both $\text{TiO}_2\text{-NP}$ (SS) and $\text{TiO}_2\text{-NT}$ (IS) photocatalytic systems. The comparison of the k values highlights, as expected, that suspended nanoparticles of TiO_2 were much more efficient in terms of bacterial inactivation as compared to that of immobilized TiO_2 . However, TiO_2 nanotubes were still successful in inactivating both mono- and dual-species biofilms in terms of the inactivation rate. Despite the lower k values, the use of $\text{TiO}_2\text{-NT}$ (IS) is favored over $\text{TiO}_2\text{-NP}$ (SS) since it reduces the energy consumption and costs of an additional step to recover TiO_2 particles.

Significant differences ($p \leq 0.05$) between *S. Typhimurium* and

Table 1

Photocatalytic inactivation kinetic constants of mono- and dual-species biofilms for suspended ($\text{TiO}_2\text{-NP}$) (SS) and immobilized TiO_2 ($\text{TiO}_2\text{-NT}$) (IS) photocatalysts. (S) *S. Typhimurium*, (L) *L. monocytogenes*. Kinetic constant (k , min^{-1}) obtained according to the Chick–Watson log-linear model. SD: ± 0.005 . Significant differences ($p \leq 0.05$) have been indicated with a different uppercase capital letter, with “A” bearing the lowest value.

Biofilm, Photocatalyst	k (min^{-1})
Mono- (S), $\text{TiO}_2\text{-NP}$ (SS)	0.030 ^C
Mono- (L), $\text{TiO}_2\text{-NP}$ (SS)	0.043 ^D
Mono- (S), $\text{TiO}_2\text{-NT}$ (IS)	0.023 ^{AB}
Mono- (L), $\text{TiO}_2\text{-NT}$ (IS)	0.014 ^A
Dual- (S), $\text{TiO}_2\text{-NP}$ (SS)	0.030 ^C
Dual- (L), $\text{TiO}_2\text{-NP}$ (SS)	0.090 ^E
Dual- (S), $\text{TiO}_2\text{-NT}$ (IS)	0.016 ^{AB}
Dual- (L), $\text{TiO}_2\text{-NT}$ (IS)	0.019 ^{AB}

L. monocytogenes photocatalytic inactivation when forming mono- and dual-species biofilms onto borosilicate glass surfaces were observed when applying a suspended photocatalytic treatment. As the kinetic constant values demonstrated (Table 1), the Gram-positive *L. monocytogenes* showed a significantly higher sensitivity to photocatalytic inactivation when co-cultured ($p \leq 0.05$). This might be explained by competitive interactions established between Gram-negative and Gram-positive bacteria when they are co-cultured. For example, some authors have reported, testing Gram-negative *S. Typhimurium* strains, that *S. Typhimurium* bacteria exhibited shorter generation times than those of Gram-positive *S. aureus* under co-culturing [22,23,27,28]. This extended lag time of Gram-positive bacteria is likely to provide an advantage to *S. Typhimurium* in covering surfaces and developing biofilms. Nevertheless, no differences in terms of initial bacterial colonization onto borosilicate glass surfaces were revealed between the two strains ($p \leq 0.05$). Hence, further research is required to understand which factors may cause some competitive interactions between the two strains. This competition may explain such high and unexpected photosensitivity of *L. monocytogenes* when co-cultured.

On the contrary, according to k values, when TiO₂-NT (IS) surfaces were used, no significant differences ($p > 0.05$) in photocatalytic inactivation of *L. monocytogenes* were observed neither when co-cultured nor when single-cultured. But it did show high photosensitivity when co-cultured. These observations confirm what was previously discussed on the competitive interactions and, moreover, underline that the surface, where the biofilm grows, plays a key role in the resistance of biofilms against photolytic and photocatalytic disinfection.

In terms of photocatalytic inactivation rate, the photocatalytic system with suspended TiO₂ gave rise to the highest inactivation rate according to the kinetic constant values. However, it must be remarked that immobilized TiO₂ enabled to reach a viable biofilm cell density reduction of 3–4 log₁₀ CFU/cm² for both *L. monocytogenes* and *S. Typhimurium*, for the mono- and dual-species biofilms. Based on this finding, this immobilized photocatalytic system seems to be more promising in terms of inactivation.

4. Conclusions

This work presents the evaluation of the efficiency of a photocatalytic treatment for inactivation of dual-species biofilms using an immobilized photocatalyst, and an equivalent suspended system. Tested biofilms were developed by (a combination of) Gram-negative and Gram-positive bacterial strains, using the mono-species biofilms as a reference.

Interestingly, under dual-species conditions, the simultaneous presence of both Gram-negative and Gram-positive bacteria strongly decreased the resistance of the Gram-positive *L. monocytogenes* cells to photolytic and photocatalytic inactivation when grown onto borosilicate glass surfaces for the suspended photocatalyst (TiO₂-NP) (SS) in comparison to the mono-species *L. monocytogenes*. For the Gram-negative *S. Typhimurium* cells, no significant differences in resistance were observed between the mono- and dual-species communities grown onto borosilicate glass surfaces. When grown onto TiO₂-NT (IS) surfaces for the immobilized photocatalyst, mono- and dual-species biofilms did not exhibit noticeable differences in terms of photocatalytic inactivation according to the kinetic constant values, but Gram-positive strains again showed increased photosensitivity when co-cultured. Thus, the results revealed that interspecies interactions did have a significant effect on the resistance of the cells to photocatalytic treatment depending on the growth surface of biofilms.

The high photocatalytic activity of immobilized TiO₂ observed for disinfection of mono- and dual-species bacterial biofilms, is of high relevance for water treatment and food processing applications. Thus, the use of immobilized TiO₂ photocatalysis increases the operating efficiency, making it feasible to deploy photocatalytic technology in real-life scenarios. Moreover, it contributes to sustainable wastewater

treatment and food processing technology.

Declaration of Competing Interest

The authors declare that they have no known competing financial interests or personal relationships that could have appeared to influence the work reported in this paper.

Acknowledgments

The authors gratefully acknowledge the financial support of the Spanish State Research Agency (AEI) and the Spanish Ministry of Science, Innovation, and Universities through the project CALYPSOL-ATECWATER (RTI2018-097997-B-C33) and Comunidad de Madrid through the program REMTAVARES (P2018/EMT-4341). Cristina Pablos also acknowledges the Spanish Ministry of Science, Innovation, and Universities (MICIU) for its mobility grant through the program José Castillejo for young researchers (CAS18/00414). This research was also funded by the KU Leuven Research Council (project C24/18/046) and the Fund for Scientific Research-Flanders (projects G.0863.18 and G.0B41.21N).

Appendix A. Supplementary Data

Supplementary data to this article can be found online at <https://doi.org/10.1016/j.jphotobiol.2021.112253>.

References

- [1] J.M.C. Robertson, C. Sieberg, P.K.J. Robertson, The influence of microbial factors on the susceptibility of bacteria to photocatalytic destruction, *J. Photochem. Photobiol. A* 311 (2015) 53–58.
- [2] C. Buck, N. Skillen, P.K.J. Robertson, J.M.C. Robertson, Influence of bacterial, environmental and physical factors in design of photocatalytic reactors for water disinfection, *J. Photochem. Photobiol. A* 366 (2018) 136–141.
- [3] R.A.N. Chmielewski, J.F. Frank, Biofilm formation and control in food processing facilities, *Compr. Rev. Food Sci. Food Saf.* 2 (2003) 22–32.
- [4] B. Jalvo, M. Faraldos, A. Bahamonde, R. Rosal, Antimicrobial and antibiofilm efficacy of self-cleaning surfaces functionalized by TiO₂ photocatalytic nanoparticles against *Staphylococcus aureus* and *Pseudomonas putida*, *J. Hazard. Mater.* 340 (2017) 160–170.
- [5] R.H. Pires, M.F. Brugnera, M.V.B. Zanoni, M.J.S.M. Gianninia, Effectiveness of photoelectrocatalysis treatment for the inactivation of *Candida parapsilosis* sensu stricto in planktonic cultures and biofilms, *Appl. Catal. A-Gen.* 511 (2016) 149–155.
- [6] C. Pablos, R. van Grieken, J. Marugán, B. Moreno, Photocatalytic inactivation of bacteria in a fixed-bed reactor: mechanistic insights by epifluorescence microscopy, *Catal. Today* 161 (2011) 133–139.
- [7] R. van Grieken, J. Marugán, C. Pablos, L. Furones, A. López, Comparison between the photocatalytic inactivation of Gram-positive *E. faecalis* and Gram-negative *E. coli* faecal contamination indicator microorganisms, *Appl. Catal. B Environ.* 100 (2010) 212–220.
- [8] J. You, Y. Guo, R. Guo, X. Liu, A review of visible light-active photocatalysts for water disinfection: features and prospects, *Chem. Eng. J.* 373 (2019) 624–641.
- [9] N.G. Chorianopoulos, D.S. Tsoukleris, E.Z. Panagou, P. Falaras, G.J.E. Nychas, Use of titanium dioxide (TiO₂) photocatalysts as alternative means for *Listeria monocytogenes* biofilm disinfection in food processing, *Food Microbiol.* 28 (2011) 164–170.
- [10] B. Jalvo, M. Faraldos, A. Bahamonde, R. Rosal, Antibacterial surfaces prepared by electrospray coating of photocatalytic nanoparticles, *Chem. Eng.* 334 (2018) 1108–1118.
- [11] Y. Li, Y.F. Cheng, Development of nanostructured photocatalytic coatings for antibioadhesion and self-cleaning of residual bacterial cells, *Chem. Eng.* 338 (2018) 513–525.
- [12] M. Pezzoni, P.N. Catalanoh, D.C. Delgado, R.A. Pizarro, M.G. Bellino, C.S. Costa, Antibiofilm effect of mesoporous titania coatings on *Pseudomonas aeruginosa* biofilms, *J. Photochem. Photobiol. B* 203 (2020) 111762.
- [13] M. Govaert, C. Smet, M. Baka, T. Janssens, J. Van Impe, Influence of incubation conditions on the formation of model biofilms by *Listeria monocytogenes* and *Salmonella typhimurium* on abiotic surfaces, *J. Appl. Microbiol.* 125 (2018) 1890–1900.
- [14] E. Mena, M.J. Martín de Vidales, S. Mesones, J. Marugán, Influence of anodization mode on the morphology and photocatalytic activity of TiO₂-NTs array large size electrodes, *Catal. Today* 313 (2018) 33–39.
- [15] H. Chick, An investigation of the Laws of disinfection, *J. Hyg. (Lond.)* 8 (1) (1908) 92–158.

- [16] C. Rodríguez-Melcón, Alicia Alonso-Hernando, Félix Riesco-Peláez, C. García-Fernández, C. Alonso-Calleja, R. Capita, Biovolume and spatial distribution of foodborne gram-negative and gram-positive pathogenic bacteria in mono- and dual-species biofilms, *Food Microbiol.* 94 (2021) 103616.
- [17] M. Govaert, C. Smet, J.L. Walsh, J.F.M. Van Impe, Dual-species model biofilm consisting of *Listeria monocytogenes* and *Salmonella typhimurium*: development and inactivation with cold atmospheric plasma (CAP), *Front. Microbiol.* 10 (2019) 2524.
- [18] S. Haddad, M. Elliot, T. Savard, L. Deschenes, T. Smith, T. Ells, Variations in biofilms harbouring *Listeria monocytogenes* in dual and triplex cultures with *Pseudomonas fluorescens* and *Lactobacillus plantarum* produced under a model system of simulated meat processing conditions, and their resistance to benzalkonium chloride, *Food Control* 123 (2021) 107720.
- [19] E.B. Kerekes, A. Vidács, M. Takó, T. Petkovits, C. Vágvölgyi, G. Horváth, V. L. Balázs, J. Krisch, Anti-biofilm effect of selected essential oils and main components on mono- and polymicrobial bacterial cultures, *Microorganisms* 7 (2019) 345–359.
- [20] S. van der Veen, T. Abee, Mixed species biofilms of *L. monocytogenes monocytogenes* and *Lactobacillus plantarum* show enhanced resistance to benzalkonium chloride and peracetic acid, *Int. J. Food Microbiol.* 144 (2011) 421–431.
- [21] E. Giaouris, N. Chorianopoulos, A. Doulgeraki, G.J. Nychas, Co-culture with *L. monocytogenes* within a dual- species biofilm community strongly increases resistance of *Pseudomonas putida* to Benzalkonium chloride, *PLoS One* 8 (10) (2013), e77276.
- [22] E.N. Gkana, E.D. Giaouris, A.I. Doulgeraki, S. Kathariou, G.-J. Nychas, E. Biofilm formation by *S. Typhimurium Typhimurium* and *Staphylococcus aureus* on stainless steel under either mono- or dual-species multi-strain conditions and resistance of sessile communities to sub-lethal chemical disinfection, *Food Control* 73 (2017) 838–846.
- [23] M. Iñiguez-Moreno, M. Gutiérrez-Lomelí, P.J. Guerrero-Medina, M.G. Avila-Novoa, Biofilm formation by *Staphylococcus aureus* and *S. Typhimurium spp.* under mono and dual-species conditions and their sensitivity to cetrinonium bromide, peracetic acid and sodium hypochlorite, *Braz. J. Microbiol.* 49 (2018) 310–319.
- [24] X. Li, L. Yin, G. Ramage, B. Li, Y. Tao, Q. Zhi, H. Lin, Y. Zhou, Assessing the impact of curcumin on dual-species biofilms formed by *Streptococcus mutans* and *Candida albicans*, *Microbiol. Open.* 00 (2019), e937.
- [25] M. Kostaki, N. Chorianopoulos, E. Braxou, G.J. Nychas, E. Giaouris, Differential biofilm formation and chemical disinfection resistance of sessile cells of *L. monocytogenes monocytogenes* strains under monospecies and dual-species (with *S. Typhimurium enterica*) conditions, *Appl. Environ. Microbiol.* (2012) 2586–2595.
- [26] C.H. Puga, P. Rodríguez-López, M.L. Cabo, C. San Jose, B. Orgaz, Enzymatic dispersal of dual-species biofilms carrying *L. monocytogenes* and other associated food industry bacteria, *Food Control* 94 (2018) 222–228.
- [27] J. Makovcova, V. Babak, P. Kulich, J. Masek, M. Slany, L. Cincarova, Dynamics of mono- and dual-species biofilm formation and interactions between *Staphylococcus aureus* and gram-negative bacteria, *Microb. Biotechnol.* 10 (2017) 819–832.
- [28] D.M.C. Pompermayer, C.C. Gaylarde, The influence of temperature on the adhesion of mixed cultures of *Staphylococcus aureus* and *Escherichia coli* to polypropylene, *Food Microbiol.* 17 (2000) 361–365.